# Evaluation of Peripheral Nerve Injury According to the Severity of Damage Using $^{18}$F-FDG PET/MRI in Rat Sciatic Nerve

Jong Yeol Park

Department of Dentistry

The Graduate School, Yonsei University

# Evaluation of Peripheral Nerve Injury According to the Severity of Damage Using $^{18}$F-FDG PET/MRI in Rat Sciatic Nerve

Directed by Professor Hyung Jun Kim

The Doctoral Dissertation

Submitted to the Department of Dentistry,

The Graduate School, Yonsei University

in partial fulfillment of the requirements for the degree of

Ph.D. in Dental Science

Jong Yeol Park

December 2022

This certifies that the Doctoral Dissertation
of Jong Yeol Park is approved.

Thesis Supervisor: Hyung Jun Kim

Thesis Committee Member : In-Ho Cha

Thesis Committee Member : Dongwook Kim

Thesis Committee Member : Eun-Joo Choi

Thesis Committee Member : Jung-Woo Nam

The Graduate School
Yonsei University

December 2022

Acknowledgment

지도 교수님으로서 큰 가르침과 사랑을 주신 김형준 교수님께 가장 먼저 깊은 감사를 드립니다. 바쁘신 와중에도 논문 심사를 맡아 주시고 지도를 해주신 차인호, 김동욱, 최은주, 남정우 교수님께 감사드립니다. 구강악안면외과의사로서 지금의 제가 있을 수 있도록 많은 가르침을 주신 존경하는 이상휘, 강정완, 정영수, 남웅, 정휘동, 박진후, 김준영 교수님께도 깊은 감사를 드립니다.

박사 학위를 마칠 수 있도록 긴 시간 동안 응원해주시고 격려해주신 사랑하고 존경하는 아버지, 어머니께 감사드립니다. 그리고 늘 귀감이 되는 형과 형수님, 귀여운 예원이와 주원이, 사랑하는 여동생에게도 고마움을 전합니다. 구강악안면외과 수련을 함께 했던 동기 김영관, 김진규, 하태욱, 후세인 알파델 이브라힘, 그리고 의국원들에게도 고마움을 전합니다. 어려울 때 자기 일처럼 도와준 친구 광호와, 주영이에게 고마움을 전합니다.

지난 세월을 눈동자와 같이 보호해주시고 바른길로 인도해주신 하나님께 감사드립니다. 이 박사 논문으로 이제 저의 연구 역량을 키워가는 여정을 시작하였습니다. 앞으로도 교실의 발전에 보탬이 되도록 힘써 노력하겠습니다.

2022년 12월

박종열

Table of contents

# LIST OF FIGURES

LIST OF TABLES

**Abstract**

# Evaluation of Peripheral Nerve Injury According to the Severity of Damage Using $^{18}$F-FDG PET/MRI in Rat Sciatic Nerve

Jong Yeol Park

*Department of Dentistry*

*The Graduate School, Yonsei University*

(Directed by Professor Hyung Jun Kim)

Reports suggest a high incidence of nerve injuries following tooth extraction or implant surgery and various methods have attempted to evaluate the severity of nerve damage. The two-point discrimination and the pin prick test are widely used techniques; however they rely on subjective sensations and were not able to accurately represent the damaged area. A previous experiment revealed that $^{18}$F-FDG PET/MRI could detect nerve damage in a peripheral nerve injury model.

This study aimed to evaluate peripheral nerves according to different severity of damage using $^{18}$F-FDG PET/MRI in rat sciatic nerve.

Eighteen rats were equally divided into three groups in this experiment: 30 seconds crushing injury group (G1), 2 minutes crushing injury group (G2), and 5 minutes crushing injury group (G3). The severity of nerve damage was measured in the third week after the crush injury using the following evaluation methods: paw withdrawal threshold (RevWT), maximum standardized uptake values on PET/MRI imaging (SUVR), and immunohistochemical analysis (IntR).

There were significant differences between G1 and G3 in both SUVR and IntR($p=0.008$, $p=0.0386$). There were no significant differences in both SUVR and IntR between G2 and G3 and no significant difference in RevWT among the three groups. There was a statistical difference in SUVR between G1 and G2 ($p=0.0135$). However, there was no significant difference in IntR between G1 and G2.

The severity of nerve damage for both 2 and 5 minutes of crush injury was more than that for 30 seconds crush injury. There was no significant difference in the severity of nerve damage between 2 and 5 minutes of crush injury. While RevWT represented the limitations of neurosensory tests in clinical practice, SUVR showed better results in differentiating the severity of nerve damage. Although PET/MRI did not show results consistent with the immunohistochemistry in all respects, this study demonstrated that the severity of nerve damage as assessed by PET/MRI increased with a longer crushing time. PET/MRI showed potential as an objective diagnostic tool in this peripheral nerve injury model. If research is supplemented through further experiments, PET/MRI can be used as an effective diagnostic modality.

---

Keywords: Peripheral nerve injury, Neuropathic pain, Crushing injury, Positron emission tomography (PET)

# Evaluation of Peripheral Nerve Injury According to the Severity of Damage Using $^{18}$F-FDG PET/MRI in Rat Sciatic Nerve

Jong Yeol Park

Department of Dentistry

The Graduate School, Yonsei University

(Directed by Professor Hyung Jun Kim)

## I. Introduction

Peripheral nerve injury can results from clinical accidents and trauma and accounts for 2.8% of all trauma cases.[1] Nerve tissue and repair are associated with various changes such as the development of edema, free oxygen release, and inflammatory changes. Recently, nerve injuries have been reported following dental procedures, such as tooth extraction or implant surgery.[2] When a nerve is

damaged, a diagnosis must be made to determine the severity of damage, to predict the recovery period, and to assess whether surgery should be performed or not.. The need for research to evaluate these points has been noted. Studies are needed to evaluate the degree of damage and monitor the recovery process. Various methods, such as two-point discrimination and the pin prick test, have been attempted to evaluate the severity of nerve damage. However, these techniques rely on subjective sensations and may not accurately represent the damaged area. Historical assessment is the most definitive method for evaluating nerve injury. However, it has limited clinical application as it is invasive and requires tissue sections. Several studies have attempted to develop accurate and objective methods to determine the severity and location of nerve damage.

First, digital infrared thermal imaging (DITI) is a good method of evaluating inflammation and blood flow. The second is ultrasonography (US), which is a good diagnostic method to obtain information about nerve hypertrophy and intraneural vascularization. Finally, positron emission tomography (PET) has an advantage of identifying the area of nerve damage. However, it is difficult to accurately visualize the damaged area with this modality. Therefore, Purohit et al. recommended using other modalities such as US or magnetic resonance imaging (MRI) when using PET imaging.[3]

There have been few systematic *in vivo* nerve injury studies (as mentioned in a previous paper).[4] Rat models are considered ideal for nerve damage and regeneration due to ease of availability and similarities in the appearance of nerve bundles compared with humans.[5] Moreover, the rat model provides a nerve trunk with sufficient length and space for surgical manipulation and allows the investigator to apply direct trauma.[6] The previous paper showed the effectiveness of PET/MRI in diagnosing peripheral nerve damage with two well-known nerve models: the chronic constriction injury (CCI) and crushing injury models.[4] PET/MRI showed significant findings consistent with those of histological and functional tests. The findings suggested that the experiment should be further verified by evaluating peripheral nerve damage according to its severity. This previous experiment also confirmed that $^{18}$F-FDG PET/MRI detected nerve damage in their peripheral nerve injury model. This study aimed to evaluate peripheral nerve damage according to differences in the severity of damage using $^{18}$F-FDG PET/MRI in rat model of sciatic nerve damage. As an objective indicator to compare $^{18}$F-FDG PET/MRI results, immunohistochemistry (IHC) and the paw withdrawal threshold (PWT) test, which are clinical neurosensory tests, were also performed.

# II. Materials and methods

## 1. Animal model

Eighteen male Sprague-Dawley rats (7 weeks old; weight: 200-250 g) were used. Rats were provided daily food and water, weighed once a week, and allowed to acclimatize to a specially-made customized modular holder cage before weight measurement. All animal protocols were approved by the Institutional Animal Use and Care committee of the Department of Laboratory Animal Resources, Yonsei Bio-Medical Research Institute, Yonsei University College of Medicine, Korea.

## 2. Experimental design

The subjects were divided into 3 groups (n=6, respectively). All surgical procedures were performed on the left sciatic nerve. In the crushing injury model, the first group received 30 seconds of crushing time, the second group 2 minutes, and the last group 5 minutes. A Curved hemostat (12.5cm HB0515; HEBU, Germany) was used to apply crush injury. The starting point of the curve was used as the reference point for the crusher. (Fig. 1) The clamping force between the tips of the tongs was about 40 N, and the width was 3 mm. Groups were set up as below. (Table 1)

**Table 1. Experimental groups divided into three groups**

| Group | Crushing time |
|---|---|
| 1 | 30 seconds |
| 2 | 2 minutes |
| 3 | 5 minutes |

### 3. Surgical procedure

Under respiratory anesthesia with isoflurane (Forane; JW, Korea), the left thigh area was shaved and cleaned with 10% povidone-iodine. A 2-cm skin incision was made on 0.5 cm posterior from the femur. The fascia of the biceps femoris and the gluteus superficialis were exposed to access the sciatic nerve by blunt dissection through the intermuscular space. Approximately 15 mm of the nerve was carefully freed from the surrounding tissue using micro-pincettes (Fig 1). With a curved hemostat, crushing injuries were applied to the experimental groups using three different durations described previously. Surgical sites were closed layer-by-layer with 4-0 absorbable synthetic braided suture(Vicryl; Polygalactin 910; Ethicon, INC., a Johnson and Johnson company, Sommerville, NJ, USA) for muscle and fascia and 5-0 non-absorbable synthetic monofilament suture (Nylon; AILEE Co., Busan, Korea) for the skin. After performing the PWT test before surgery and 1, 2, and 3 weeks after surgery and taking PET/MRI at 3 weeks after surgery, all animals were sacrificed by $CO_2$ inhalation. Left sciatic nerves were harvested for histological analysis.

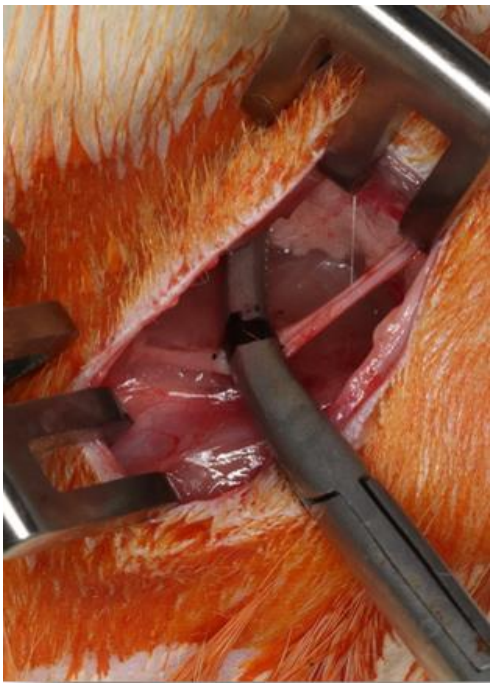

**Figure 1. Crush injury by locking with a curved hemostat for 0.5, 2, and 5 minutes**

**4. Pain behavior assessment**

Pain behavior assessments were performed four times (pre-operative, 1 week after the operation, 2 weeks after the operation, and 3 weeks after the operation) in the right hind paw (control) and the left hind paw (experimental site) with abundant time period. Both hind paws were measured thrice, and the mean value was used. Manual von Frey filament (BIO-VF-M; Bioseb Inc., Vitrolles, France) the gold standard for determining mechanical thresholds in rats, was used for the paw withdrawal threshold test (PWT), and it shows force according to its size (Fig. 2). The rats were positioned in the customized modular holder cage and wait for 15 minutes for acclimatization.[7] A Monofilament was applied perpendicularly to the plantar surface of the hind paw until it bent, delivering a constant pre-determined force for 2 to 5 seconds (Fig. 3, 4). The response was considered positive if the rats exhibited paw withdrawal during filament application or immediately after filament removal. The plantar surface of the hind paw was the most commonly used area for testing and the response was observed via a wire-gated floor. If a response was shown in any particular value, the mouse was re-examined with a value one step below the value, and if there was no response to the value, the particular value was recorded as result.


**Figure 2. PWT test with Von Frey filament**


**Figure 3. A monofilament was applied perpendicular to the platar surface of the hind paw.**

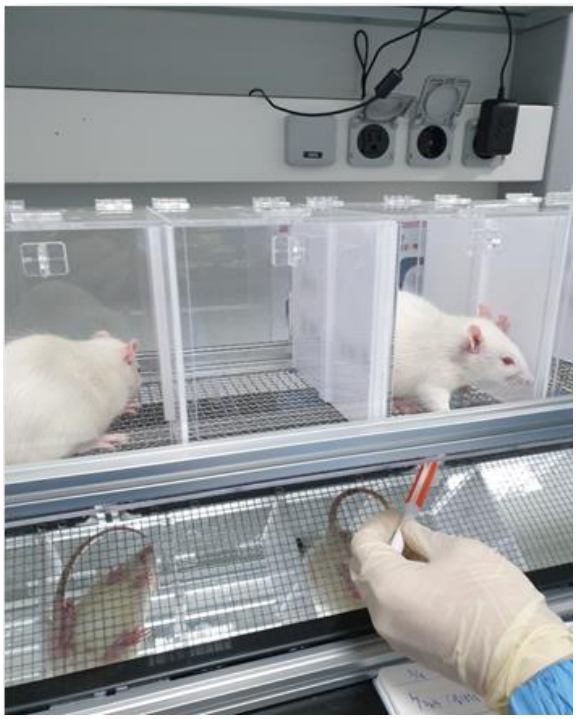

**Figure 4. Rats were allowed to acclimatize to a specially made customized modular holder cage before weight measurement.**

**5. PET/MRI imaging**

All rats fasted for 12 hours the day before 3 weeks of post operation (becoming violent and dangerous after 16 hours of fasting) for PET. Animals underwent sequential small-animal PET(Inveon PET; Siemens, Germany) and small-animal MRI(Bruker 9.4 T 20-cm-bore MRI system; Biospec 94/20 USR; Bruker, Ettlingen, Germany). A customized PET table similar to an MRI table was prepared and used to facilitate image superimposition. A dose between 1.000-1.070 uCi was injected intravenously. 1-hour dynamic scans of the thigh were obtained, and T2-weighted rapid acquisition with relaxation enhancement (RARE) images of the thighs (repetition time [TR] = 2300 ms; echo time [TE] = 11 ms; slice thickness = 1 mm, acquisition matrix = 192×192; acquisition FOV 55×55 $mm^2$) were obtained at postoperative 3 weeks. Co-registration of PET and MRI was performed using AMIDE image analysis software (amide.exe1.0.4; https://amide.sourceforge.net). The MRI images indicated the anatomic location of the sciatic nerves and the placement of the regions of interest (ROIs). Spherical-shaped ROIs, about 6 mm in diameter, were set on the nerve injury site and the opposite side. For quantitative analysis of PET signals, the maximum standardized uptake values (SUVmax) of the ROIs were calculated using OsiriX image analysis software (Pixmeo, Geneva, Switzerland). The ratio of the SUV (SUVR) from two different regions within the same PET image (from a target and a reference region) was also calculated to eliminate differences between the animals as follows:

$$SUVR = \frac{SUV_{target}}{SUV_{reference}} = \frac{SUV_{left\ ROI}}{SUV_{right\ ROI}}$$

After the PET and MRI scans were performed, the rats were sacrificed the next day (after 24 hours, considering the drug's half-life) to prepare tissue sections.

### 6. Histology and immunohistochemistry

All harvested left sciatic nerves were fixed in 4% paraformaldehyde for 24 hours immediately after sacrifice and they were embedded in paraffin with threads indicating their orientation. For each specimen, three cross-sections (4 μm thickness) taken in the middle of the injury site, 1 mm proximal, and 1 mm distal to the injury site were mounted on slides and stained with hematoxylin and eosin (H&E) for histological and immunohistochemistry analysis. (Fig. 5)

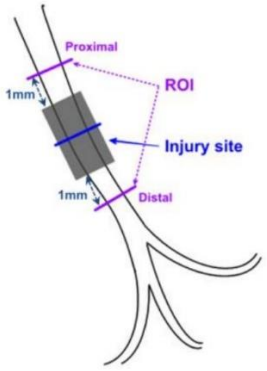


**Figure 5. Specimen ROIs[4] -** Injury site and 1 mm proximal and 1 mm distal to the injury site mounted on slides

For immunostaining, ROI, proximal and distal areas were fixed with 4% paraformaldehyde (PFA), permeabilized with 0.5% Triton-100 (Sigma-Aldrich), and blocked with 1% bovine serum albumin (Sigma-Aldrich). For the staining of cell markers, samples were incubated with specific primary antibodies: Anti S-100 beta antibody (Abcam ab52642 10 ul) for 2 hours at room temperature, washed with PBS thrice, and then Goat anti Secondary staining was performed with rabbit IgG H & L (Abcam ab 205718, 500 ug) for immunohistochemistry. Tissue slides obtained by staining were photographed using a Zeiss LSM780, confocal microscope system (Zeiss, KBSI(Korean Basic Science Institute) in Seoul center). This analysis was performed on three randomly selected non-overlapping microscope fields. The evaluated part covered two-thirds of the whole part. All slide pictures were selected by an expert blinded to the rat group. The intensity obtained from the microscope varied according to the degree of staining. The intensity was analyzed using ImageJ software.[8] The analysis protocol was implemented according to the paper described by Crowe and Yue (especially sections on Threshold DAB (3-diaminobenzidine tetrahydrochloride) stained IHC (Immunohistochemistry) image and Quantify the DAB signal in the IHC image).[9] The following is the protocol described by Crowe and Yue. (Fig. 6)

Quantify the DAB signal in the IHC image

1. Go to “Analyze” and select “Set Measurements.”

2. A “Set Measurement” pop-up window will open. Select the “Area,” “Mean grey value”, and “Display Label” boxes and leave all other boxes unchecked. “Area” will give the size of the IHC image. “Mean grey value” represents the quantified signal and “Display Label” gives the information on the image name being quantified.

3. Select “Okay” in the Set Measurement window. These options only need to be set once for the first image and will be remembered for all other future images measured.

4. Go to “Analyze” and select “Measure.” Note: A shortcut for measuring the signal is “CTL + M.”

5. A “Results” window will pop up giving the name of the image (Label), the size of the image (Area), and the average pixel intensity of the IHC image (Mean)

6. Copy the results to an Excel file for later analysis.

Zhao et al. observed that greater damage correlated with more active regeneration of Schwann cells. Therefore I expected that the intensity of S-100, a Schwann cell biomarker, express strongly.[10] Herein, the development of strong intensity was considered a positive response to the S-100 antibody. Experimental data were obtained with 3 randomly selected sections. The average intensity measured in three sections was used for the result value. The brown-stained part was recorded as a positive reaction of the S-100 antibody. The mean gray value was evaluated using ImageJ software particle analysis; the mean value was the average of intensity in the selection, which meant raw integrated density/pixel number (Fig. 6). Dubovy reported that Schwann cells distal to the crushed sciatic nerve showed increased immunostaining for proinflammatory and anti-inflammatory cytokines.[11] Schwann cells distal to the crushed sciatic nerve were expected to increase as greater damage correlates with higher S-100 intensity values. To compensate for the difference between individual rats, the S-100 intensity of the distal part of the ROI was divided by the S-100 intensity of the proximal part of the ROI. The corresponding value was expressed as IntR.

$$IntR = \frac{Mean\ Gray\ Value_{distal}}{Mean\ Gray\ Value_{proximal}}$$

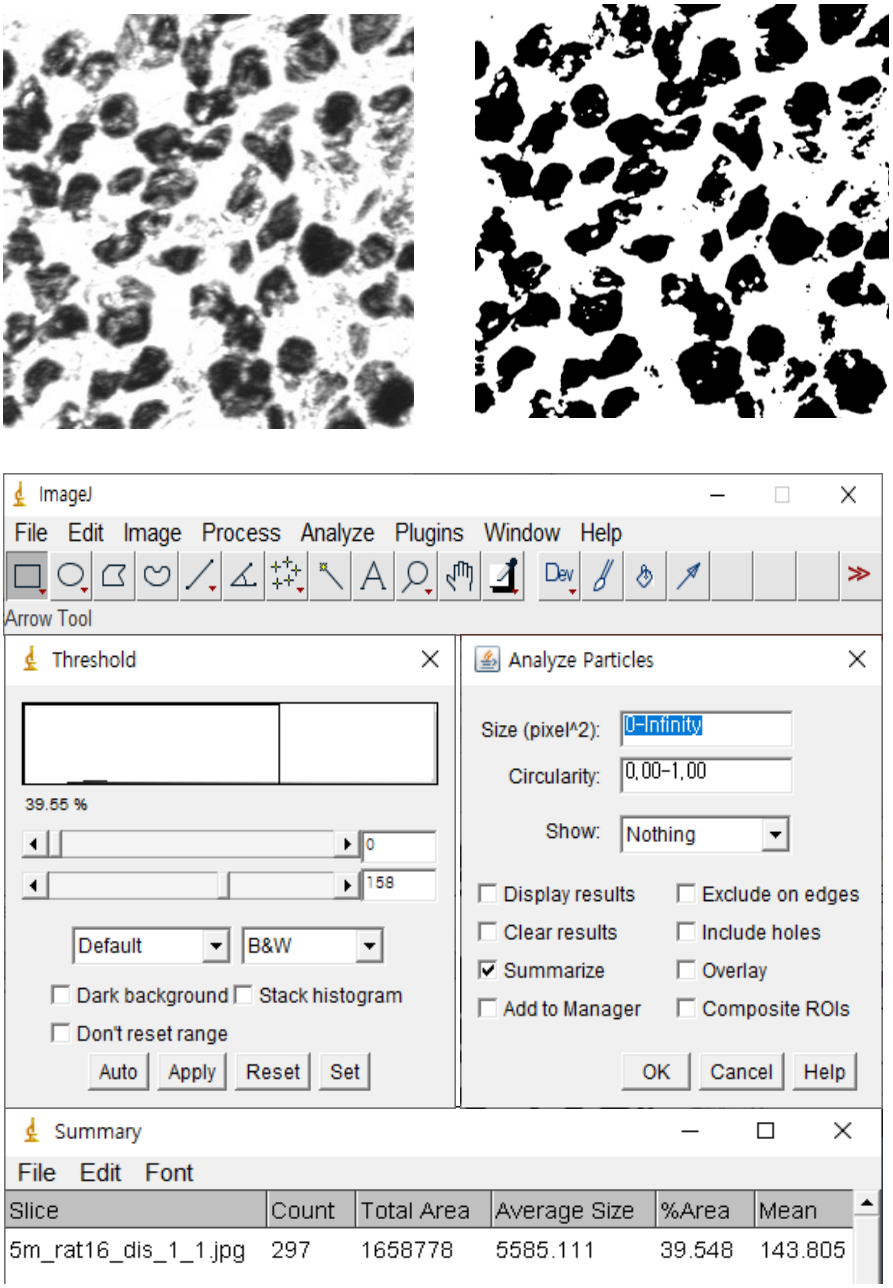


**Figure 6. Photograph showing how S-100 intensity was analyzed with ImageJ software.**

### 7. Statistics

Statistics were analyzed using GraphPad Prism (Version 8.0.0 for Windows, GraphPad Software, San Diego, California, USA, www.graphpad.com). Shapiro-Wilk was used to determine whether each group had a normal distribution. Because all the results did not follow the normal distribution in the normality test, and the number of rats was six in each group, non-parametric test methods were conducted. The independent sample Kruskal-Wallis test was performed to examine whether there was a significant difference in the result values between each group. The Kruskal-Wallis test was conducted to determine the difference between the three methods. Dunn's multiple comparison test was used to determine which groups were significantly different. A $P<0.05$ was considered statistically significant.

# III. Result

## 1. Assessment of pain

First, the Kruskal-Wallis test was used for the three groups to determine whether there was a significant difference between each result. Kruskal-Wallis test showed no significant difference between PWT test results (Table 2). Table 2 showed that the right hind paw (intact side) groups had lower standard deviation values than the left hind paw group (injured side).

Overall, G2 and G3 showed more severe hypoesthesia in the second week than in the first week; however, hypoesthesia recovered significantly in the third week, possibly due to significant nerve recovery. The level of hypoesthesia appeared to increase with an increased intensity of nerve damage. However, in third week, all three groups showed almost complete recovery (Fig. 7). However, the right hind paw graph showed that G1, 2, and 3 were constant without significant statistical difference (Fig. 8).

**Table 2. Kruskal-Wallis test results of PWT on three groups (Mean, (SD))**

| **Group** | **n** | **pre-op** | | **post-op 1wk** | | **post-op 2wk** | | **post-op 3wk** | |
|---|---|---|---|---|---|---|---|---|---|
| | | **Left** | **Right** | **Left** | **Right** | **Left** | **Right** | **Left** | **Right** |
| 1 | 6 | 29.667 (16.727) | 27.717 (13.066) | 162.55 (115.483) | 44.283 (14.203) | 138.117 (125.471) | 37.55 (24.672) | 68.65 (55.672) | 44.383 (22.677) |
| 2 | 6 | 27.85 (16.597) | 26.5 (12.518) | 193.667 (116.744) | 42.5 (20.817) | 178.45 (133.229) | 34.383 (21.479) | 89.55 (53.482) | 48.067 (11.027) |
| 3 | 6 | 32.117 (16.258) | 27.767 (7.59) | 184.783 (127.36) | 36 (24.809) | 188.884 (121.821) | 34.6 (20.215) | 68.017 (28.014) | 43.19 (21.801) |
| total | 18 | 29.878 (15.63) | 27.328 (10.659) | 180.333 (113.504) | 40.928 (19.525) | 168.484 (121.338) | 35.511 (20.907) | 75.406 (45.713) | 45.183 (18.207) |
| *p value* | | *0.874* | *0.771* | *0.706* | *0.654* | *0.32* | *0.98* | *0.511* | *0.937* |

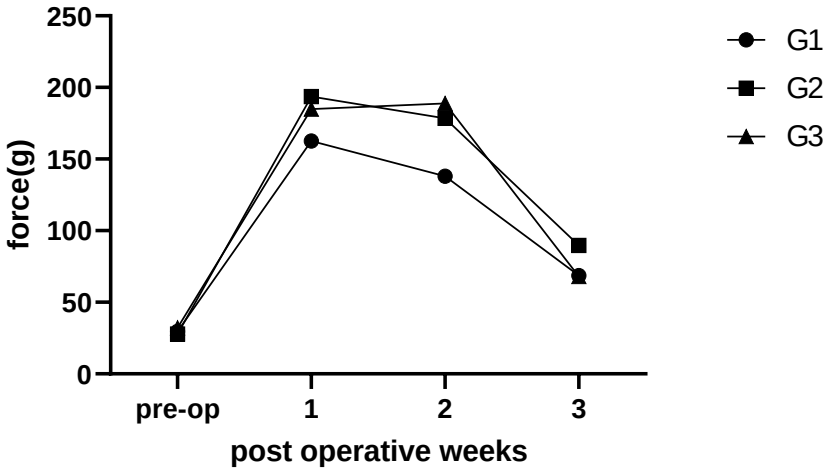


**Figure 7. Left hind PWT test** – Hypoesthesia was seen compared to pre-op. G1 showed hypoesthesia in the 1st week and recovered rapidly with the passage of time. Both G2 and G3 showed hypoesthesia pattern in the 1st week and 2nd week, and recovered significantly in the 3rd week.

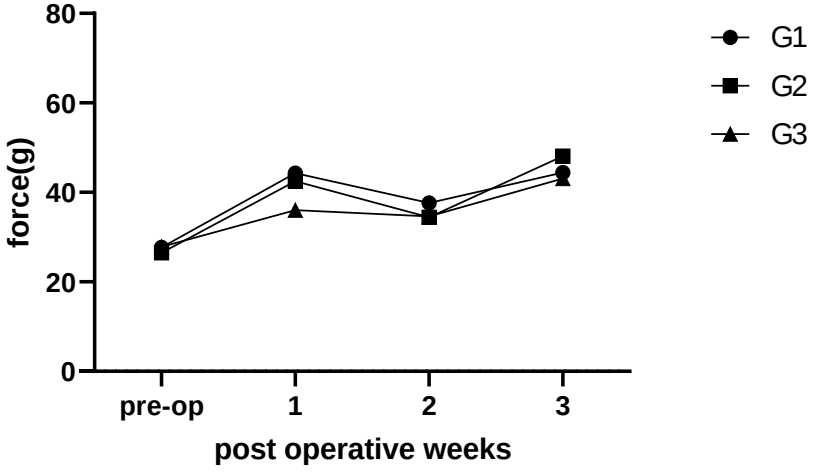


**Figure 8. Right hind PWT test showed no significant differences among G1, G2, and G3.**

Withdrawal threshold values were revised to compensate for different conditions of individual rats (such as sensitivity, nervousness, fear, adaptation, and blunting) before comparison between variables at postoperative 3 weeks in the three groups. Revised withdrawal threshold values (RevWT) were calculated as follows:

$$RevWT = \frac{Withdrawal\ thresholds\ value\ of\ injured\ side}{Average\ of\ withdrawal\ threshold\ values\ of\ intact\ sides\ in\ each\ group}$$

For example, the G1 preL value was 26.0 g, and the average of the withdrawal threshold value of intact sides for G1 was 27.7 g. Then, the RevWT value was 26.0 g / 27.7 g = 0.983064 (preL/R) (Tables 3, 4, 5).

The Kruskal-Wallis test demonstrated that all G1, G2, and G3 showed significant difference between values (p=0.0144, p=0.0237, p=0.005 respectively). In Dunn's multiple comparisons test, G1 represented only pre-op and the first week showed significant difference (p=0.0469). However, G2 showed a significant difference between pre-op and second week (p=0.0226). G3 showed a significant difference between pre-op and second week (p=0.0112) (Fig. 9, 10, 11).

When changing from one filament to the next, the increase in force was not linear, and the gap between filaments was very large. As the force increased, the thickness of the filament also increased. Therefore, it was not possible to accurately measure the force alone. Herein, value of pressure, which is the force per unit area of the filament, was calculated according to Aesthesio's precision tactile sensory evaluator data chart (Fig. 12). However, there was no significant difference among the groups for pressure (Table 6).

**Table 3. G1 RevWT** (Kruskal-Wallis test p=0.014)

| | **preL/R** | **1wL/R** | **2wL/R** | **3wL/R** |
|---|---|---|---|---|
| s11 | 0.938 | 1.355 | 1.598 | 0.840 |
| s12 | 0.747 | 1.400 | 1.297 | 0.840 |
| s13 | 0.552 | 1.655 | 1.598 | 1.352 |
| s14 | 1.346 | 4.065 | 1.598 | 1.352 |
| s15 | 0.675 | 6.775 | 7.989 | 4.056 |
| s16 | 2.165 | 6.775 | 7.989 | 0.840 |
| **Mean** | 1.070 | 3.671 | 3.678 | 1.547 |
| **SD** | 0.603 | 2.608 | 3.341 | 1.254 |

**Table 4**. **G2 RevWT** (Kruskal-Wallis test p=0.024)

| | **preL/R** | **1wL/R** | **2wL/R** | **3wL/R** |
|---|---|---|---|---|
| s21 | 0.781 | 2.353 | 1.745 | 1.248 |
| s22 | 0.442 | 1.772 | 1.416 | 1.525 |
| s23 | 0.566 | 2.040 | 1.803 | 0.776 |
| s24 | 0.842 | 7.059 | 8.725 | 1.248 |
| s25 | 1.838 | 7.059 | 8.725 | 3.745 |
| s26 | 1.838 | 7.059 | 8.725 | 2.636 |
| **Mean** | 1.051 | 4.557 | 5.190 | 1.863 |
| **SD** | 0.626 | 2.747 | 3.875 | 1.113 |

**Table 5. G3 RevWT** (Kruskal-Wallis test p=0.006)

| | preL/R | 1wL/R | 2wL/R | 3wL/R |
|---|---|---|---|---|
| s31 | 0.673 | 1.667 | 2.506 | 0.603 |
| s32 | 0.745 | 1.353 | 2.118 | 1.130 |
| s33 | 0.673 | 2.778 | 2.118 | 2.012 |
| s34 | 1.343 | 8.333 | 8.671 | 1.392 |
| s35 | 1.343 | 8.333 | 8.671 | 2.320 |
| s36 | 2.161 | 8.333 | 8.671 | 2.012 |
| **Mean** | 1.157 | 5.133 | 5.459 | 1.578 |
| **SD** | 0.586 | 3.538 | 3.521 | 0.650 |

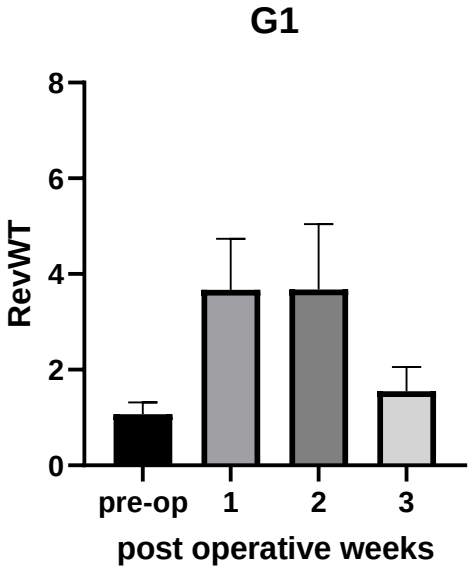


**Figure 9. G1 RevWT for postoperative 3 weeks**

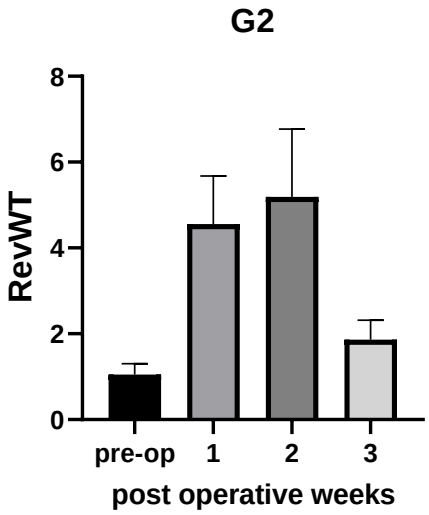


**Figure 10. G2 RevWT for postoperative 3 weeks**

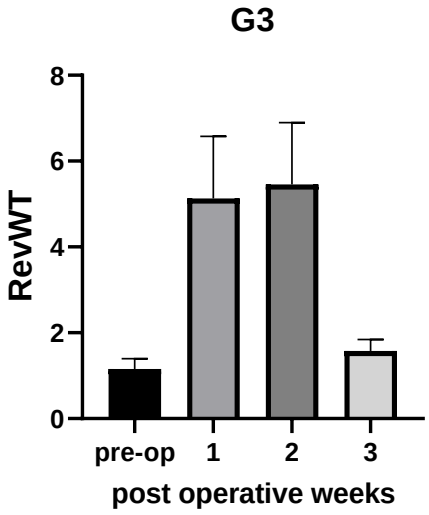


**Figure 11. G3 RevWT for postoperative 3 weeks**

Aesthesio®
Precision Tactile Sensory Evaluator

**Aesthesio® Precision Tactile Sensory Evaluator Data Chart**

| Color | Evaluator Size | Catalog Item Number | Target Force (grams) | Target Force* (milliNewtons) | Theoretical Pressure LBS/Sq. Inch | Theoretical Pressure Grams/Sq. mm |
|---|---|---|---|---|---|---|
| Green | 1.65 | 514001 | 0.008 | 0.08 | 3.59 | 2.53 |
| | 2.36 | 514002 | 0.02 | 0.20 | 6.23 | 4.39 |
| | 2.44 | 514003 | 0.04 | 0.40 | 7.01 | 4.93 |
| | 2.83 | 514004 | 0.07 | 0.70 | 7.85 | 5.53 |
| Blue | 3.22 | 514005 | 0.16 | 1.6 | 12.5 | 8.77 |
| | 3.61 | 514006 | 0.40 | 3.9 | 22.9 | 16.1 |
| Purple | 3.84 | 514007 | 0.60 | 5.9 | 26.1 | 18.4 |
| | 4.08 | 514008 | 1.0 | 9.8 | 34.6 | 24.4 |
| | 4.17 | 514009 | 1.4 | 13.7 | 39.6 | 27.9 |
| | 4.31 | 514010 | 2.0 | 19.6 | 39.0 | 27.4 |
| Red | 4.56 | 514011 | 4.0 | 39.2 | 57.2 | 40.3 |
| | 4.74 | 514012 | 6.0 | 58.8 | 74.8 | 52.6 |
| | 4.93 | 514013 | 8.0 | 78.4 | 87.6 | 61.7 |
| | 5.07 | 514014 | 10 | 98.0 | 97.0 | 68.3 |
| | 5.18 | 514015 | 15 | 147 | 117 | 82.0 |
| | 5.46 | 514016 | 26 | 255 | 151 | 106 |
| | 5.88 | 514017 | 60 | 588 | 200 | 141 |
| | 6.10 | 514018 | 100 | 980 | 274 | 193 |
| | 6.45 | 514019 | 180 | 1760 | 316 | 222 |
| Orng | 6.65 | 514020 | 300 | 2940 | 416 | 292 |

*Calculated rounded numbers. (Conversion factor 9.80665)

**Figure 12. von Frey filament unit conversion table from force to pressure** (LBS/sq. inch)

**Table 6. Kruskal-Wallis test results of converted PWT among groups (Mean, (SD))**

| Group | n | pre-op | | post-op 1wk | | post-op 2wk | | post-op 3wk | |
|---|---|---|---|---|---|---|---|---|---|
| | | **Left** | **Right** | **Left** | **Right** | **Left** | **Right** | **Left** | **Right** |
| **1** | 6 | 104.8 | 103.1 | 208.7 | 124.1 | 189.4 | 111.3 | 138 | 122.2 |
| | | (21.9) | (18.79) | (70.7) | (15.3) | (79.6) | (32.9) | (29.3) | (29.5) |
| **2** | 6 | 100,8 | 102.3 | 234.8 | 119.9 | 215.5 | 125.4 | 163.8 | 128 |
| | | (23.74) | (19.72) | (63.4) | (27.4) | (84) | (41.4) | (40.2) | (12.5) |
| **3** | 6 | 108.3 | 102.9 | 223.2 | 112.2 | 228.1 | 111.6 | 153.5 | 121.6 |
| | | (20.68) | (12.67) | (78.3) | (32.6) | (70.3) | (25.1) | (33.3) | (27.1) |
| total | 18 | 104.7 | 102.7 | 222.2 | 118.7 | 211 | 116.1 | 151.8 | 123.9 |
| | | (21.04) | (16.3) | (67.7) | (25.1) | (75.3) | (32.5) | (34.2) | (22.9) |
| *p value* | | *0.897* | *0.989* | *0.706* | *0.654* | *0.32* | *0.737* | *0.399* | *0.937* |

## 2. PET/MRI evaluation

MRI enabled clear visualization of the anatomy, and PET/MRI fusion images showed sciatic nerve injury sites as hot spots (Fig. 13). Longer injury time showed a correlation with a higher SUVR (Fig. 14). For the quantitative analysis of PET image, SUVmax and SUVR of ROIs were calculated using OsiriX image analysis software (Table 7). SUVR demonstrated a significant difference in the Kruskal-Wallis test results for the three groups (Table 8). In Dunn's multiple comparisons test, G1 showed a significant difference from G2 (p=0.0135) and also from G3 (p=0.0080). However, there was no significant difference between G2 and G3 (p=>0.9999). Although G2 and G3 had different crushing injury times, there was no statistically significant difference (Fig. 15).

**Table 7. Imaging analysis on PET/MRI**

| Group | | 1 | | | | | | 2 | | | | | | 3 | | | | | |
|---|---|---|---|---|---|---|---|---|---|---|---|---|---|---|---|---|---|---|---|
| Rat(n=18) | | 1 | 2 | 3 | 4 | 5 | 6 | 1 | 2 | 3 | 4 | 5 | 6 | 1 | 2 | 3 | 4 | 5 | 6 |
| SUV max (g/ml) | Lt. | 1.09 | 1.17 | 0.95 | 0.95 | 1.09 | 0.95 | 1.08 | 0.4 | 0.92 | 1.17 | 1.04 | 0.96 | 1.51 | 0.86 | 1 | 1.06 | 1.16 | 0.94 |
| | Rt. | 0.91 | 0.96 | 0.72 | 0.77 | 0.93 | 0.78 | 0.69 | 0.3 | 0.65 | 0.82 | 0.74 | 0.69 | 1.1 | 0.63 | 0.69 | 0.74 | 0.71 | 0.67 |
| *SUVR (Lt/Rt)* | | *1.2* | *1.22* | *1.31* | *1.23* | *1.16* | *1.22* | *1.56* | *1.35* | *1.42* | *1.43* | *1.41* | *1.38* | *1.37* | *1.37* | *1.45* | *1.43* | *1.65* | *1.41* |

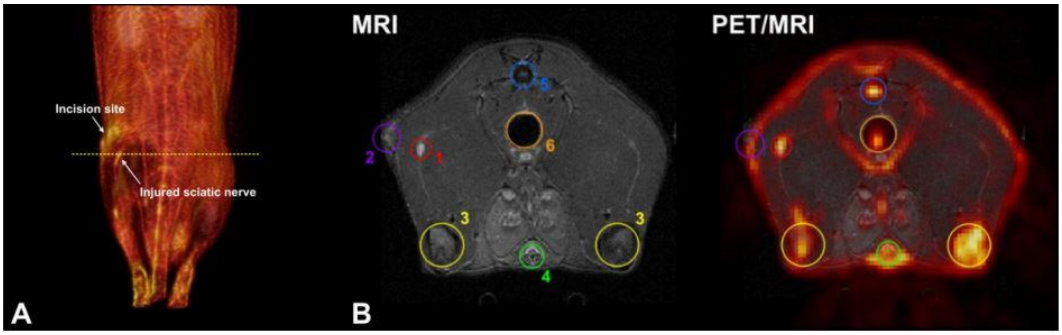


**Figure 13. Imaging analysis on PET/MRI**.[4] The yellow dotted line illustrates the location of PET/MRI slices. a Labeled anatomical structures on PET/MRI. 1=nerve injury site, 2=incision site, 3=knee joint, 4=penile urethra, 5=vein and tail, 6=rectum

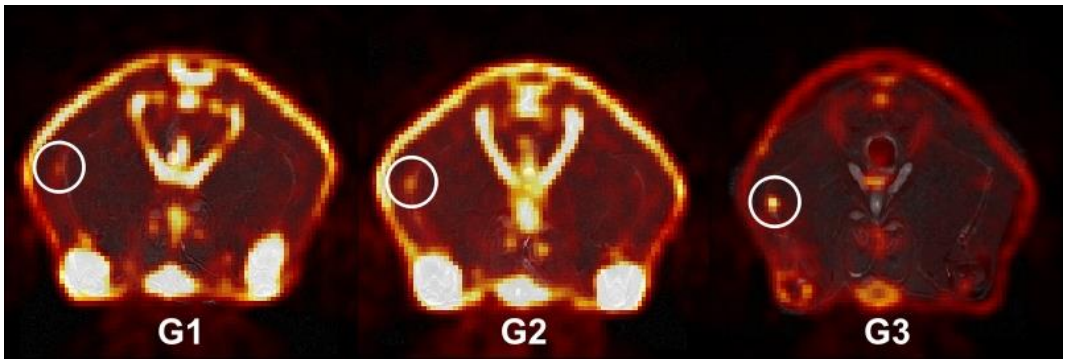


**Figure 14. PET/MRI fusion images** (These white circles indicate the ROI of injured sites of left sciatic nerves.)

**Table 8. Results of PET/MRI evaluation(Mean, (SD))**

| **Group** | **n** | **SUVR** |
|---|---|---|
| 1 | 6 | 1.225<br>(0.049) |
| 2 | 6 | 1.426<br>(0.074) |
| 3 | 6 | 1.447<br>(0.105) |
| total | 18 | 1.366<br>(0.127) |
| *p value* | | *0.001* |

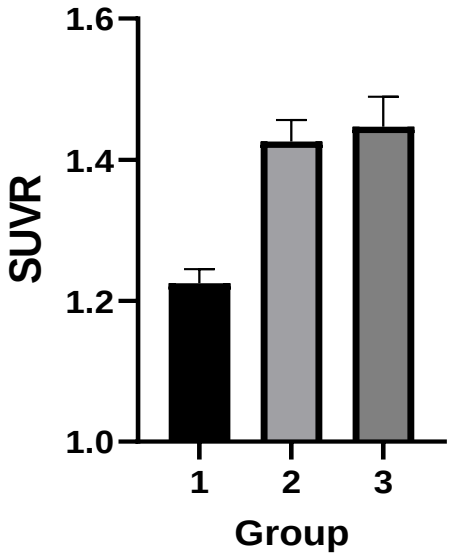


**Figure 15. SUVR result for the three groups** – Although G2 and G3 had different crushing injury times, there was no statistically significant difference.

### 3. Histology and immunohistochemistry

Hemorrhage was observed in the tissue slides. Diameter and epineurium thickness was relatively increased. Dense myelinated axons surrounded with perineural epithelium were visible in all sections. Some slides showed intact and vital cellular features. In contrast, some other slides showed folded tissues, and tissue condition was not well-organized due to errors in tissue processing. Some slides showed fragmentation, atrophy of myelin and axons, swollen neuronal bodies, and interstitial fibrosis.

Here S-100 immunohistochemistry was used to determine the severity of damage by calculating S-100 intensity (Fig. 16). With S-100 stained slides, the intensity was analyzed using ImageJ software.[8] The analysis protocol was implemented with according to a study by Crowe and Yue (Fig. 16).[9] Kruskal-Wallis test showed a significant difference between groups ($p=0.038$). Dunn's multiple comparison test was conducted among groups, and the p-values were 0.8385, 0.0386, 0.4792, 1vs2, 1vs3, 2vs3 respectively (Table 9, Fig. 17). There were no significant differences between G1 and G2 and between G2 and G3. However, there was a significant difference between G1 and G3 (Fig. 18).

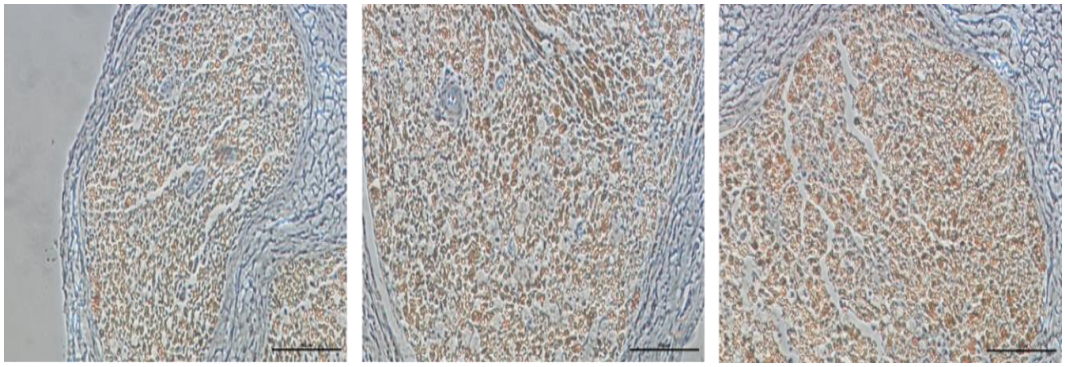

**Figure 16. Histological images of G1, G2, and G3**. (Scale bar indicates 100 μm) – The brown-stained part is a positive reaction of the S-100 antibody.

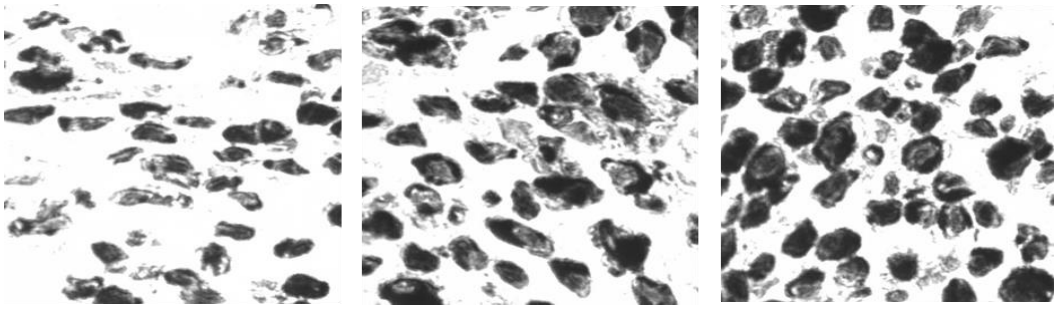

**Figure 17. IntR analysis of G1, G2, and G3**

**Table 9. IntR result** – There was a significant difference between G1 and G3 (Dunn's multiple comparisons test p = 0.0386) and no significant difference between G1 and G2, G2 and G3)

| Group | IntR | |
|---|---|---|
| | ***Mean*** | ***SD*** |
| 1 | 0.95615 | 0.164563 |
| 2 | 1.0773493 | 0.070061 |
| 3 | 1.1496442 | 0.071055 |
| total | 1.061048 | 0.101893 |
| ***p value*** | ***0.0378*** | |

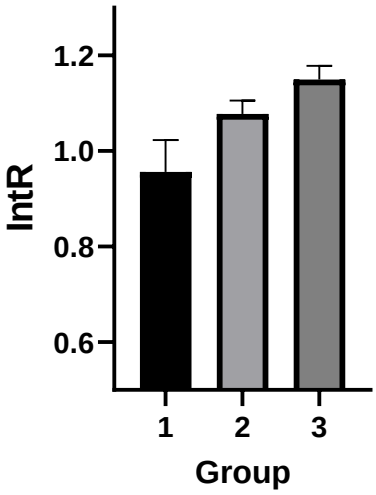


**Figure 18. IntR result** - There was a significant difference between G1 and G3 (*p = 0.0386*). However, there were no significant differences between G1 and G2 and between G2 and G3.

### 4. Comparison between assessment methods

In RevWT, there was no significant difference among groups in the third week (Kruskal-Wallis test p= 0.7668). However, there was a significant difference between G1 and G2, and between G1 and G3 (Dunn's multiple comparisons test p = 0.001, 0.001, respectively) in SUVR. However, there was no significant difference between G2 and G3 (p > 0.99) in SUVR. Lastly, there was a significant difference between G1 and G3 (Dunn's multiple comparisons test p=0.0386) and no significant difference between G1 and G2, G2 and G3 (p = 0.8385, 0.4792) in IntR (Table 10, Fig. 19).

**Table 10. Comparison between assessment methods**

| | |
|---|---|
| ***RevWT*** ***(p= 0.767)*** | No significant difference among three groups 3 weeks after surgery. |
| ***SUVR*** ***(P =0.005)*** | Significant difference between G1 and G2 and between G1 and G3<br>*(Dunn's multiple comparisons test p= 0.0135, 0.0080 respectively)*<br>No significant difference between G2 and G3 |
| ***IntR*** ***(P =0.038)*** | Significant difference between G1 and G3<br>*(Dunn's multiple comparisons test p = 0.0386)*<br>No significant difference between G1 and G2, G2 and G3 |

**RevWT (revised withdrawal threshold value) = left value / right mean value*
**SUVR = maximum SUV on left ROI/ maximum SUV on right ROI*
**IntR = distal Mean Gray Value / proximal Mean Gray Value*
(p values are Kruskal-Wallis test values.)

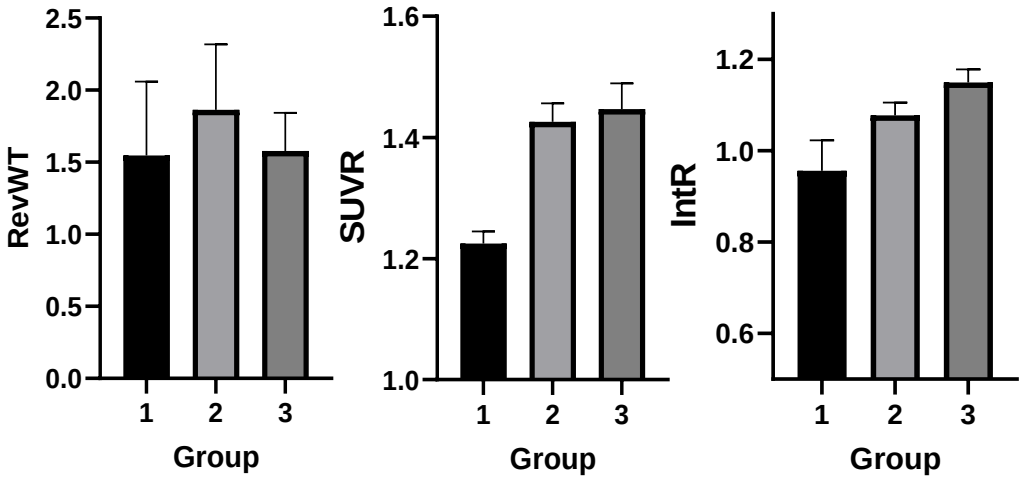


**Figure 19. Result graphs of three assessment methods**

# IV. Discussion

Peripheral nerve injury produces loss of sensory and motor function, resulting in critical economic and psychological issues and diminished quality of life. Common causes of peripheral nerve injuries are traffic accidents, firearm injuries, chemical injuries, cutting tool injuries and crush.[1] Nerve injuries may also result from dental procedures, such as extraction, implantation, minor operation, root canal treatment (chemical injury) and trauma.[2] There is no doubt that an accurate diagnosis leads to accurate treatment planning. However, these diagnoses are based on the patient's subjective symptoms. An objective and accurate diagnosis can help achieve successful treatment outcomes. To my knowledge, this is the first study to evaluate peripheral nerve injury according to the severity of damage using $^{18}$F-FDG PET/MRI in rat sciatic nerve.

The nerve damage model can be divided into three groups according to crushing time. Alvites et al. reported that in most studies, crush time was different for each paper. There was no standardized protocol of crushing time varying from 15 seconds to 2 hours.[12-19] An et al. attempted to objectify the damage intensity by varying the number of notches on the forceps and the location of the pinching forceps.[20] In this experiment, I tried to examine the difference in the sciatic nerve according to the crushing time.

Other papers have used various crush load tools, such as Jeweler’s forceps, Kocher's forceps, pincers, mosquito forceps and aneurysmal clips.[19] Also, serrated and non-serrated forceps were used without distinction. In this experiment, a curved hemostat with serration was used; however, the serration was in a certain direction, and crush injury could be applied only to a specific nerve part by clamping at one time. Thus, there may be a nerve part where crush injury was not applied. Thus it was difficult to inflict more than a certain level of injury. Beer et al. used a non-serrated clamp for standardizing the nerve crush model to ensure that the pressure on the injury site was uniformly transmitted.[21] Future studies should develop a consistent crush injury model using tools, such as non-serrated hemostats, applying crush injury by turning 90 degrees after crushing once, or applying crush by changing the angle by 90 degrees with two hemostats.

However, there were several limitations in measuring the PWT with von Frey filament. One limitation of the von Frey filament test was that it did not allow for differentiation between pain

response and routine bodily grooming/itching. Mason et al., stated that it was important to note the length of time for specific behavior to differentiate between pain and grooming. Typically, the pain response is one swipe after filament application; however, the grooming motion tends to be longer and can last from a few seconds to a few minutes. If the grooming/itching behavior is indistinguishable from irritability, it is best not to record it as a positive response.[22] When manual filament was used, there was possibility that the subjective interpretation of the experimenter may be intervened. Therefore, both hind paws were measured three times, and the mean value was used for analysis.

When changing from one filament to the next, the force increase was not linear, and the force gap between filaments was very large. For example, after using a 60 g filament, the next filament size force was 100, then 180, then 300. As the force increased, the thickness of the filament became thicker, and it was not possible to obtain accurate measurements for force alone. Therefore I calculated the value in pressure, which is the force per unit area of the filament. Results showed no significant difference between force and pressure. However, future studies should use pressure units instead force to obtain more precise data. In view of these points, PWT test showed subjective results similar to the neurosensory test in clinical practice.

Nevertheless, the withdrawal threshold result was consistent with other research results. Roman et al. demonstrated hypoesthesia by time in the first, second, and third weeks; the peak was in the first and second weeks, and hypoesthesia gradually improved and recovered from the third week.[16] Histological analysis was also consistent with other studies. In a sciatic nerve injury model by Zhang, immunohistological finding showed Schwann cell proliferation over time, with a peak in the first and second weeks, followed by decrease in the third week.[23]

Histological analysis was conducted using the immunohistochemistry method. Schwann cells play vital roles in peripheral nerve regeneration. Schwann cells play a major role in managing distinct functional modalities between macrophage procedures.[24] However, the identification by conventional histological methods is difficult. Schwann cells can be identified using an antibody against the S-100 protein. Detection of Schwann cells by immunochemical staining is considered a positive indicator of nerve regeneration.[25] In parallel, the accumulated S-100 protein indicates the proliferation of sciatic nerve Schwann cells. Proliferating Schwann cells promote the sustained regeneration and functional recovery of sciatic nerves.[26] Zhao et al. used S-100 as a Schwann cell

marker to compare the effect of decimeter wave therapy on the proliferation of Schwann cells after nerve injury.[10] S-100 protein expression increases when Schwann cells proliferate. Therefore, high levels of S-100 protein indicate active Schwann cells proliferation, which promotes nerve regeneration.

S-100 may serve as a marker for the proliferation of Schwann cells in sciatic nerve regeneration research.[27] Wang et al. reported that ginsenoside Re significantly increased S-100 expression in Schwann cells to promote rat sciatic nerve regeneration.[28] The proliferation of neural sheath cells was also demonstrated by a quantitative increase in the specific antigen, S-100 protein.[29] Moreover, the amount of S-100 immunoreactivity in myelinated fibers appeared to correlate directly with the thickness of the myelin sheath formed by Schwann cells.[30] Pan et al. indicated that expression of immunoreactivity of S-100 as a late marker to evaluate the intensity of nerve regeneration.[12] In this experimental study, S-100 intensity was measured and the values (IntR) were compared with SUVR results.

Many studies have focused on non-invasive diagnostic tools using imaging methods, such as ultrasonography (US) showing nerve hypertrophy and intraneural vascularization.[31,32] The quantity and quality of nerve damage have been studied using diffusion tension imaging).[33] Moreover, radioactive tracers in PET scan have been used to assess the severity of nerve damage. PET alone has some advantages and disadvantages. Although it can indicate nerve damage, it is difficult to determine the exact location. In particular, in this experiment, PET/MRI fusion was used to combine the limitations of PET and the advantages of MRI. Purohit et al. stated that researchers should be aware of several specific patterns of FDG uptake and they suggested contrast-enhanced CT, US, or MRI together to prevent errors in PET interpretation.[3] This study used the PET/MRI fusion image method to obtain metabolic $^{18}$F-FDG PET images with a more precise anatomical evaluation with MRI.

Results confirmed that PET imaging and IHC values increased as nerve-crushing time increased. Both imaging and histological results showed a significant difference between 30 seconds and 5 minutes of crush injury. However, there was no significant difference between 2 and 5 minutes in both results. One reason is that a curved hemostat with sufficient strength produce a crush injury even in 2 minutes; therefore, there was no difference between 2 and 5 minutes. To give a difference in time through crush injury, it is worth considering reducing crushing time to 1 minute or giving a

difference in the ratchet of clamping. Conversely, investigator should consider methods other than clamping for crush durations of more than 2 minutes. Another study reported that crush injury through clamping could not produce more severe injuries, such as neurotmesis.[20] Therefore, no significant difference was expected between 2 and 5 minutes of crush injury.

Unlike imaging analysis, histological result showed no statistically significant difference between 30 seconds and 2 minutes. This finding could result in a subjective interpretation of histological characteristics. In addition it may not be consistent to obtain reliable histological data because the professional technology for each process are required for histological analysis.[34] Therefore, this study used computer-aided IHC analysis to minimize subjectivity in interpretation. The biggest advantage of IHC unlike immunofluorescence (IF), is that IHC stating is permanent with no change in color. Moreover, tissue morphology is clearly visible, simplifying interpretation. With IF, fluorescence eventually disappears; therefore, photographing and scans are necessary to maintain record.[35] A disadvantage is that fluorescence can be automatically generated when using formalin-fixed paraffin-embedded tissue (FFPE), seen in autofluorescent elements, such as, collagen, elastin, neutrophils and blood vessels. Therefore, it is very important to restore slides that are not stained with isotype controls and use frozen sections instead of FFPE tissues. An advantage of IF is that it allows visualization of cell populations at once through various staining technique on one slide. Recently, IF has been widely used in immune-oncology research. Fluorescence quantification can provide better visualization and more sensitive results for future experiments.[36,37]

Different severity of crush injury is very important experimentally. This study aimed to quantify SUVR according to the severity of injury in a rat sciatic nerve injury model in PET/MRI. When a rat receives any damage, it will be possible to objectify the severity of damage by taking PET imaging. As a result it will be also possible to predict how long it will take to recover if long-term data is accumulated.

There are errors and difficulties in obtaining measurements with manual filaments. However, these aspects are similar to neurologic examinations currently performed in clinical practice and may vary depending on the measurer's subjective interpretation and the subject's sensory diversity, which are current limitations. With advancements in image capture systems, non-communicating and non-stimulus evoked pain evaluations allow more accurate and useful comuputer-aided.[38] The sciatic nerve can be evaluated by analyzing the toe angle during the gait stance duration, ankle kinematic,

and gait through video recording of motion evaluation without considering the method of evaluation by applying pressure.[19] The analysis is technically complex and necessitates appropriate equipment. However, more precise results can be obtained if this method is also used for further research.

As there were only 6 rats in each group, there were differences in numerical values. Moreover, all the statistic results did not show significant differences. Future studies should include at least 30 rats and use statistical methods with the parametric test to yield more sensitive and accurate results. Moreover, PET/MRI can be used to quantify the severity of damage and predict prognosis. Thus PET/MRI can objectively evaluate treatment efficacy when studying new drugs used for neuropathic pain.

Doctors often face the challenges of defining diagnosis and prognosis based only on the patient's subjective symptoms. Patients have difficulties describing the symptoms of their sensory numbness and felt frustrated.. However, objective tools can diagnose nerve injury, predict prognosis, and provide treatment satisfaction for doctors and patients.

# V. Conclusion

Following the previous study, this study demonstrated that the severity of nerve damage as assessed by PET/MRI increased with an increased nerve-crushing time. Although PET/MRI did not show results consistent with the histological analysis in all respects, PET/MRI showed potential as an objective diagnostic tool for assessing this peripheral nerve injury model, even considering the errors in the experimental design and the results of the PWT test, which represents a clinical neurosensory test. If this research is supplemented through further experiments, PET/MRI may be used as an effective diagnostic modality.

# References

1 Kalender, A. M. *et al.* Effect of Zofenopril on regeneration of sciatic nerve crush injury in a rat model. *J Brachial Plex Peripher Nerve Inj* 4, 6, doi:10.1186/1749-7221-4-6 (2009).

2 Ahn DK, P. M. Animal Models for Orofacial Neuropathic Pain. *Hanyang Med Rev.* 2, 107-115 (2011).

3 Purohit, B. S. *et al.* FDG-PET/CT pitfalls in oncological head and neck imaging. *Insights Imaging* 5, 585-602, doi:10.1007/s13244-014-0349-x (2014).

4 Nam, J. W., Lee, M. J. & Kim, H. J. Diagnostic Efficacy of (18)F-FDG PET/MRI in Peripheral Nerve Injury Models. *Neurochem Res* 44, 2092-2102, doi:10.1007/s11064-019-02846-w (2019).

5 Fullarton, A. C., Lenihan, D. V., Myles, L. M. & Glasby, M. A. Obstetric brachial plexus palsy: a large animal model for traction injury and its repair. Part 1: age of the recipient. *J Hand Surg Br* 25, 52-57, doi:10.1054/jhsb.1999.0337 (2000).

6 Tos, P. *et al.* Chapter 4: Methods and protocols in peripheral nerve regeneration experimental research: part I-experimental models. *Int Rev Neurobiol* 87, 47-79, doi:10.1016/S0074-7742(09)87004-9 (2009).

7 Chaplan, S. R., Bach, F. W., Pogrel, J. W., Chung, J. M. & Yaksh, T. L. Quantitative assessment of tactile allodynia in the rat paw. *J Neurosci Methods* 53, 55-63, doi:10.1016/0165-0270(94)90144-9 (1994).

8 Schneider, C. A., Rasband, W. S. & Eliceiri, K. W. NIH Image to ImageJ: 25 years of image analysis. *Nat Methods* 9, 671-675, doi:10.1038/nmeth.2089 (2012).

9 Crowe, A. R. & Yue, W. Semi-quantitative Determination of Protein Expression using Immunohistochemistry Staining and Analysis: An Integrated Protocol. *Bio Protoc* 9, doi:10.21769/BioProtoc.3465 (2019).

10 Zhao, F. *et al.* Electric stimulation and decimeter wave therapy improve the recovery of injured sciatic nerves. *Neural Regen Res* 8, 1974-1984,

doi:10.3969/j.issn.1673-5374.2013.21.006 (2013).

11 Dubovy, P., Klusakova, I. & Hradilova Svizenska, I. Inflammatory profiling of Schwann cells in contact with growing axons distal to nerve injury. *Biomed Res Int* 2014, 691041, doi:10.1155/2014/691041 (2014).

12 Pan, H. C. *et al.* Escalated regeneration in sciatic nerve crush injury by the combined therapy of human amniotic fluid mesenchymal stem cells and fermented soybean extracts, Natto. *J Biomed Sci* 16, 75, doi:10.1186/1423-0127-16-75 (2009).

13 Feng, X. & Yuan, W. Dexamethasone enhanced functional recovery after sciatic nerve crush injury in rats. *Biomed Res Int* 2015, 627923, doi:10.1155/2015/627923 (2015).

14 Kato, N. *et al.* Critical role of p38 MAPK for regeneration of the sciatic nerve following crush injury in vivo. *J Neuroinflammation* 10, 1, doi:10.1186/1742-2094-10-1 (2013).

15 Ramli, D., Aziz, I., Mohamad, M., Abdulahi, D. & Sanusi, J. The Changes in Rats with Sciatic Nerve Crush Injury Supplemented with Evening Primrose Oil: Behavioural, Morphologic, and Morphometric Analysis. *Evid Based Complement Alternat Med* 2017, 3476407, doi:10.1155/2017/3476407 (2017).

16 Pavic, R., Pavic, M. L., Tvrdeic, A., Tot, O. K. & Heffer, M. Rat sciatic nerve crush injury and recovery tracked by plantar test and immunohistochemistry analysis. *Coll Antropol* 35 Suppl 1, 93-100 (2011).

17 Ghayour, M. B., Abdolmaleki, A. & Behnam-Rassouli, M. The Effect of Memantine on Functional Recovery of the Sciatic Nerve Crush Injury in Rats. *Turk Neurosurg* 27, 641-647, doi:10.5137/1019-5149.JTN.16792-15.1 (2017).

18 Khullar, S. M., Brodin, P., Messelt, E. B. & Haanaes, H. R. The effects of low level laser treatment on recovery of nerve conduction and motor function after compression injury in the rat sciatic nerve. *Eur J Oral Sci* 103, 299-305, doi:10.1111/j.1600-0722.1995.tb00030.x (1995).

19 Alvites, R. Peripheral nerve injury and axonotmesis: State of the art and recent advances. *Cogent Medicine* 5: 1466404 (20 April 2018).

20 An, Y., Yan, H. X., Zhao, J. N., Yang, X. M. & Yan, J. T. Evaluation methods of a rat

sciatic nerve crush injury model. *J Integr Neurosci* 21, 91, doi:10.31083/j.jin2103091 (2022).

21 Beer, G. M., Steurer, J. & Meyer, V. E. Standardizing nerve crushes with a non-serrated clamp. *J Reconstr Microsurg* 17, 531-534, doi:10.1055/s-2001-17755 (2001).

22 Mason, B. N., Avona, A., Lackovic, J. & Dussor, G. Dural Stimulation and Periorbital von Frey Testing in Mice As a Preclinical Model of Headache. *J Vis Exp*, doi:10.3791/62867 (2021).

23 Zhang, P. *et al.* The immunohistological observation of proliferation rule of Schwann cell after sciatic nerve injury in rats. *Artif Cells Blood Substit Immobil Biotechnol* 36, 150-155, doi:10.1080/10731190801932132 (2008).

24 Ehmedah, A. *et al.* Effect of Vitamin B Complex Treatment on Macrophages to Schwann Cells Association during Neuroinflammation after Peripheral Nerve Injury. *Molecules* 25, doi:10.3390/molecules25225426 (2020).

25 Carriel, V., Garzon, I., Campos, A., Cornelissen, M. & Alaminos, M. Differential expression of GAP-43 and neurofilament during peripheral nerve regeneration through bio-artificial conduits. *J Tissue Eng Regen Med* 11, 553-563, doi:10.1002/term.1949 (2017).

26 Wang, C. Z. *et al.* Low-level laser irradiation improves functional recovery and nerve regeneration in sciatic nerve crush rat injury model. *PLoS One* 9, e103348, doi:10.1371/journal.pone.0103348 (2014).

27 Wang, H. *et al.* Matrix metalloproteinase 7 promoted Schwann cell migration and myelination after rat sciatic nerve injury. *Mol Brain* 12, 101, doi:10.1186/s13041-019-0516-6 (2019).

28 Wang, L. *et al.* Ginsenoside Re Promotes Nerve Regeneration by Facilitating the Proliferation, Differentiation and Migration of Schwann Cells via the ERK- and JNK-Dependent Pathway in Rat Model of Sciatic Nerve Crush Injury. *Cell Mol Neurobiol* 35, 827-840, doi:10.1007/s10571-015-0177-7 (2015).

29 So Hak Chung, S. D. K., Young Ho Kwon, Jung Hwan Son, Sun Yong Baek. Morphological Changes in the peripheral Nerve after Crush Injury. *Kosin Medical Journal* 15, 14~19 (2000).

30 Mata, M., Alessi, D. & Fink, D. J. S100 is preferentially distributed in myelin-forming Schwann cells. *J Neurocytol* 19, 432-442, doi:10.1007/BF01188409 (1990).

31 Goedee, H. S. *et al.* High resolution sonography in the evaluation of the peripheral nervous system in polyneuropathy--a review of the literature. *Eur J Neurol* 20, 1342-1351, doi:10.1111/ene.12182 (2013).

32 Telleman, J. A., Grimm, A., Goedee, S., Visser, L. H. & Zaidman, C. M. Nerve ultrasound in polyneuropathies. *Muscle Nerve* 57, 716-728, doi:10.1002/mus.26029 (2018).

33 Martin Noguerol, T., Barousse, R., Socolovsky, M. & Luna, A. Quantitative magnetic resonance (MR) neurography for evaluation of peripheral nerves and plexus injuries. *Quant Imaging Med Surg* 7, 398-421, doi:10.21037/qims.2017.08.01 (2017).

34 Wolf, J. C. & Maack, G. Evaluating the credibility of histopathology data in environmental endocrine toxicity studies. *Environ Toxicol Chem* 36, 601-611, doi:10.1002/etc.3695 (2017).

35 Im, K., Mareninov, S., Diaz, M. F. P. & Yong, W. H. An Introduction to Performing Immunofluorescence Staining. *Methods Mol Biol* 1897, 299-311, doi:10.1007/978-1-4939-8935-5_26 (2019).

36 Rizzardi, A. E. *et al.* Quantitative comparison of immunohistochemical staining measured by digital image analysis versus pathologist visual scoring. *Diagn Pathol* 7, 42, doi:10.1186/1746-1596-7-42 (2012).

37 Stagebio. *IHC or IF: Which is Best for My Study?*, <https://www.stagebio.com/blog/ihc-or-if-which-is-best-for-my-study> (2018).

38 Deuis, J. R., Dvorakova, L. S. & Vetter, I. Methods Used to Evaluate Pain Behaviors in Rodents. *Front Mol Neurosci* 10, 284, doi:10.3389/fnmol.2017.00284 (2017).

Abstract (In Korean)

# 백서 좌골신경에서 $^{18}$F-FDG PET/MRI를 이용한 말초신경 손상 정도에 따른 평가

<지도교수 김 형 준>

연세대학교 대학원 치의학과

박 종 열

치과에서는 발치나 임플란트 수술 후 발생하는 신경 손상이 많이 보고되고 있다. 이를 위해 신경 손상 정도를 평가하기 위한 다양한 방법이 시도되었다. 예를 들어 2점 식별(Two-point test)과 핀단자검사(Pin prick test)는 주관적인 감각에 의존하고 손상 부위를 정확하게 표현하지 못한다는 한계가 있었다. 이전 실험에서는 말초신경 손상 모델에서 $^{18}$F-FDG PET/MRI를 통한 진단학적 가능성을 확인하였다. 이에 본 연구의 목적은 백서 좌골신경에서 $^{18}$F-FDG PET/MRI를 이용하여 말초신경 손상 정도에 따

른 평가를 해보고자 하였다.

18마리의 쥐를 이용하여 30초 압궤 손상군(G1), 2분 압궤 손상군(G2), 5분 압궤 손상군(G3)의 3개 군으로 균등하게 나누어 실험하였다. 신경 손상의 정도는 수술 후 3주째에 다음의 평가 방법을 사용하여 측정하였다: 양측 다리의 회피역치 값(RevWT), PET/MRI 영상에서 maximum standardized uptake value (SUVmax)의 측정 및 조직형태학적 분석, IntR.

세 군 사이에 RevWT의 유의한 차이가 없었다. G1과 G3 간에 SUVR과 S-100 강도 실험에서는 모두 유의미한 차이가 있었다($p = 0.008$, $p = 0.0386$). G2와 G3 간에는 SUVR과 IntR 결과 모두 유의미한 차이가 없었다. G1과 G2 간에 SUVR 결과는 통계적 차이가 있었지만($p= 0.0135$), IntR 결과는 유의미한 차이가 없었다.

이전 연구에 이어 본 연구에서도 PET/MRI를 통해 압궤 손상 시간이 증가할수록 신경 손상의 정도가 증가함을 보였다. 조직학적 분석 결과와 약간의 차이는 있었지만, 실험 설계의 오류와 간이신경검사를 대표하는 회피역치검사 결과를 고려할 때 PET/MRI는 말초 신경 손상 모델에서 객관적인 진단 도구로서의 가능성을 보였다. 추후 실험을 통해 연구가 보완이 된다면 PET/MRI는 효과적인 진단 방법으로 활용될 수 있을 것으로 기대된다.

---

핵심되는 말: 말초신경손상, 신경병증성 통증, 압궤손상, 양전자 단층촬영(PET), 자기공명영상(MRI)